Modeling and Analyzing Per-flow Throughput in IEEE 802.11 Multi-hop Ad Hoc Networks

Lei Lei, Xinru Zhao, Shengsuo Cai, Xiaoqin Song, and Ting Zhang
College of Electronic and Information Engineering, Nanjing University of Aeronautics and Astronautics
Nanjing, 210016 - China
[e-mail: leilei@nuaa.edu.cn]
*Corresponding author: Lei Lei

Received July 17, 2016; revised August 6, 2016; accepted August 18, 2016; published October 31, 2016

Abstract

In this paper, we focus on the per-flow throughput analysis of IEEE 802.11 multi-hop ad hoc networks. The importance of an accurate saturation throughput model lies in establishing the theoretical foundation for effective protocol performance improvements. We argue that the challenge in modeling the per-flow throughput in IEEE 802.11 multi-hop ad hoc networks lies in the analysis of the freezing process and probability of collisions. We first classify collisions occurring in the whole transmission process into instantaneous collisions and persistent collisions. Then we present a four-dimensional Markov chain model based on the notion of the fixed length channel slot to model the Binary Exponential Backoff (BEB) algorithm performed by a tagged node. We further adopt a continuous time Markov model to analyze the freezing process. Through an iterative way, we derive the per-flow throughput of the network. Finally, we validate the accuracy of our model by comparing the analytical results with that obtained by simulations.

Keywords: IEEE 802.11 multi-hop ad hoc networks, per-flow throughput, fixed length channel slot, Markov chain

This work is supported in part by National Natural Science Foundation of China (No. 61572254, 61301103), Natural Science Foundation of Jiangsu Province of China (No. BK20161488, K2014041565), Fundamental Research Funds for the Central Universities of China (No. NJ20150014), and Qing Lan Project of Jiangsu Province of China.

http://dx.doi.org/10.3837/tiis.2016.10.011 **ISSN : 1976-7277**

1. Introduction

IEEE 802.11 multi-hop ad hoc networks have gained worldwide acceptance and popularity in the past decade. The mandatory contention based medium access control (MAC) protocol defined in the IEEE 802.11 standard is the Distribution Coordination Function (DCF) [1]. It employs a combination of the carrier sense multiple access with collision avoidance (CSMA/CA) and the binary exponential backoff (BEB) to resolve channel contentions among competing flows. Meanwhile, it provides two channel access modes, which are the basic access mode and the optional request-to-send/clear-to-send (RTS/CTS) handshaking mode. Although the DCF protocol was originally designed for the purely single-hop independent basic service set (IBSS) of wireless local area networks (WLAN), it has already become the de facto standard of multi-hop ad hoc networks [2].

With the increasing demand for high-speed multimedia communications [3-4], the saturation throughput performance of the wireless network has become more and more important. Consequently, considerable research attention has been focused on modeling and analyzing the saturation throughput performance of IEEE 802.11 ad hoc networks. Among them, the most significant one was done by G. Bianchi, which adopts a discrete Markov chain to model the backoff progress and derives the saturation throughput of the network by the stationary transmission probability of the node [5]. This pioneering work has also motivated substantial subsequent research.

The most important assumption taken by the Bianchi's model is that the packets collide with constant probability and collisions may only occur at the start instant of the packet transmission. Since the DCF protocol adopts the physical and virtual carrier sense mechanisms to resolve packet collisions, this assumption is reasonable in single-hop network scenarios. However, it is quite different in multi-hop network scenarios. Collisions induced by the jammers within the carrier sense range of the transmitter only occur at the start instant of the packet transmission, whereas collisions induced by the jammers hidden to the transmitter may occur during the whole packet transmission period. Meanwhile, the transmission periods of the flows in multi-hop senarios may overlaps with each other. Therefore, it is also difficult to analyze the time duration of the freezing process of the node, i.e., the time duration that the node senses the channel busy and deffers its own transmissions.

In this paper, we present a four-dimensional Markov chain model that adopts the fixed-length channel slot as the unit of time to analyze the per-flow throughput performance of IEEE 802.11 multi-hop ad hoc networks. We classify collisions occurring in the whole transmission process into instantaneous collisions and persistent collisions. The instantaneous collisions refer to the collisions that can only occur at the start of each transmission process and the collisions that persist during the whole transmission process are called the persistent collisions. We calculate the expected time interval for freezing of the backoff counter and freezing probability with the help of the continuous time Markov model in an iterative way. By means of the proposed model, the per-flow throughput performance of IEEE 802.11 multi-hop ad hoc networks is derived. Finally, we validate the accuracy of our model via extensive simulations.

The rest of the paper is organized as follows. Section 2 reviews related work. Section 3 introduces the preliminaries that are vital to the work in this paper. Section 4 presents our analytical model and derives the expressions of the conditional collision probability, the transmission probability in a generic fixed-length channel slot, and the per-flow throughput.

Validations of the analytical model are carried out in Section 5. Finally, we conclude this paper in Section 6.

2. Related Work

There have been considerable attempts to model the saturation throughput performance of the IEEE 802.11 DCF protocol. G. Bianchi [5] proposed a discrete bidimensional Markov chain to model the binary exponential backoff procedure and computed the saturation throughput of IEEE 802.11 DCF. Due to its simplicity and accuracy, the Markov chain model has become an important tool to analyze the performance of MAC protocols in wireless networks and has motivated substantial subsequent studies [6-10]. Parallel to the Markov chain models, some researchers also obtained the transmission probability with simplified backoff rule assumptions and then evaluate the performance of the MAC protocols [11-15].

Although extensive simulations have validated the accuracy of the models, they share a common assumption that all nodes have the same view of channel, which greatly simplifies the performance analysis. In a single-hop network, nodes are synchronized and the collisions only occur at the start instant of the packet transmission. However, nodes in multi-hop wireless networks cannot hear each other, which is referred to as the hidden terminal problem [16-18]. As a result, a node in a multi-hop wireless network may start its transmission while some other nodes are transmitting and thus, collisions can take place during the whole transmission process. Furthermore, due to the spatial reuse property of the wireless medium, there may coexist multiple transmissions of which the number can vary at any time and the packets may partially overlap in time. Generally speaking, modeling and analyzing performance for IEEE 802.11 multi-hop ad hoc networks remains an open issue.

Many researchers focus on the aggregate throughput or the mean throughput per node analysis in multi-hop networks [19-21]. Unfortunately, in a multi-hop wireless network, the performance of each flow may differ significantly from each other. Therefore, both the mean throughput and the aggregate throughput performance appear to be a gross metric without due details. On the other hand, per-flow throughput analysis in IEEE 802.11 multi-hop ad hoc networks has attracted wide attention. Researchers presented a continuous time Markov chain where each state is a set of links that can coexist. This method was first provided in [22] to analyze the throughput performance in CSMA/CA packet radio networks. It is also employed in [23] to study fairness issues in CSMA/CA based ad hoc networks. M. Garetto, etc. [24] proposed an analytical framework which combines the continuous time Markov chain model with Bianchi's work to capture the effect of BEB scheme. Through an iterative way, the per-flow throughput in a CSMA multi-hop wireless network was accurately predicted. The authors also use Lorenz curves and the Gini index, which are used in the economics literature to quantify a society's distribution of wealth to individuals, to evaluate the network's distribution of throughput to flows.

In [25], the authors pointed out the existing techniques which use Bianchi's notion of the variable slot inherently unable to be used in a hidden terminal scenario and propose a novel method of modeling time that uses a fixed-length channel slot as the unit of time. Although the simulation results show a very close match with the throughput, the conditional collision probability, and the transmission probability, the method proposed in [25] only intends to a simple topology where two senders communicate with one receiver and cannot apply to more complex topologies. Similar topologies were also studied in [26, 27]. The authors in [26] used two separate renewal processes to model two sets of nodes which are hidden from each other and a four-state discrete time Markov chain to model the channel activities. With the model,

the total network throughput and the individual node throughput were estimated. In [27] a parallel space-time Markov chain model with some intermediate states between any two consecutive backoff states was presented to model the interaction of nodes in the presence of hidden terminals. Through this model, the throughput performance of IEEE 802.11 DCF in multi-hop ad hoc networks was evaluated.

3. Preliminaries

3.1 Fixed Length Slot

Conventionally, researchers adopt the notion of the variable slot which is first introduced in [5]. The length of a slot depends on the channel state, e.g. a collided transmission, a successful transmission and an idle backoff slot of duration σ. The backoff slot size σ depends on the physical layer parameters accounting for the propagation delay, the time needed to switch from the receiving to the transmitting state, and the time to signal to the MAC layer the state of the channel. The classification of the channel state and the notion of variable slot are originally introduced for purely single-hop wireless networks where all nodes have a common view of the channel state. In such a fully connected network, collisions can only occur when two or more nodes transmit simultaneously. The channel becomes busy because of either a collided or a successful transmission. Hence, the time duration that the tagged node spends on the freezing procedure is for either a collided or a successful transmission. Thus, the interval of a slot can be easily obtained.

However, in a multi-hop wireless network, nodes outside the physical carrier sense range of each other can start their transmission independently and the packets may partially overlap in time. The length of the slot that includes the freezing process is thus variable. Therefore, we compute the freezing probability and expected interval of the freezing process by means of the continuous time Markov chain model and replace the time interval with a succession of fixed-length slots. Besides, the packet transmission process is also divided into a series of fixed-length slots. We view the channel as a succession of fixed length slots, of which the length equals to σ, no matter what the channel state is like. Indeed, all the performance metrics such as the transmission probability, collision probability, saturation throughput, etc. are evaluated based on the notion of the fixed length slot. In the following sections, the term slot refers to the fixed length slot without specific explanation.

3.2 Collision Zones

Here, we introduce the concepts of the instantaneous collision zone and the persistent collision zone. According to the two-ray ground propagation model, the relationship between the transmit power P_{tx} and the received power P_{rx} can be characterized as

$$P_{rx} = \frac{P_{tx} h_t^2 h_r^2 G_t G_r}{d^4}, \tag{1}$$

where h_t and h_r are the antenna heights of the transmitter and the receiver, respectively; G_t and G_r are the antenna gains of the transmitter and receiver, respectively; and d is the distance between the transmitter and the receiver. For successful reception, the signal-to-interference-plus-noise ration (SINR) at the receiver should be greater than the threshold $SINR_{rx}$. Assume all nodes have the same type of radio and the identical transmission power. Then, the transmission of a jammer located within a distance of

$$r_{co} = d\sqrt[4]{\mathrm{SINR}_{rx}} \tag{2}$$

from the receiver can collide with the current transmission. Let r_{tx}, r_{cs} and r_{co} denote the transmission range, the physical carrier sense range and the collision range, respectively. In practice, SINR_{rx} is usually set to 10dB, and r_{cs} is usually approximate to $2.2r_{tx.}$ Hence, by means of equation (2), we can conclude that the collision range of the receiver will exceeds the physical carrier sense range of the transmitter when $d>0.79r_{tx}$.

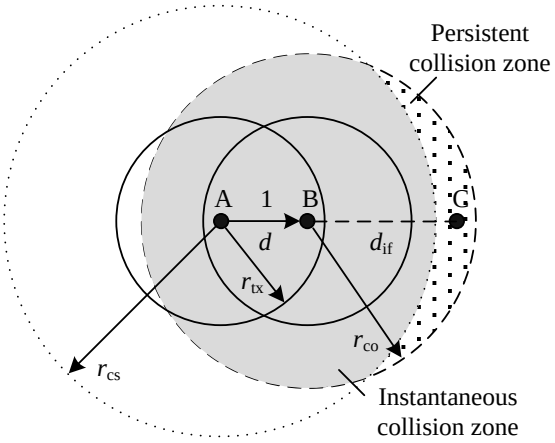

Fig. 1. Collision zones of receiver

As shown in **Fig. 1**, when the transmitter of flow 1 (node A) starts to transmit to its receiver (node B), any transmission in the collision range of node B will collide with the packet from node A. However, once node A has started its transmission, all the nodes in the physical carrier sense range of node A will sense a busy channel and then defer their transmission to avoid collisions. In other words, the collision due to the jammers that locate in both the physical carrier sense range and the collision range of node A (shown as the shaded area in **Fig. 1**) can only occur at the start instant of the transmission process of node A. Therefore, we define the instantaneous collision zone as the area within both the physical carrier sense range of the transmitter and the collision range of the receiver.

Furthermore, we illustrate the concept of persistent collision zone. As shown in Fig. 1, there may exist jammers (e.g., node C) located in the collision range of node B but outside the physical carrier sense range of node A when $d>0.79r_{tx}$. Since node C cannot sense the transmission of node A, the packet from node A can be collided at any time as long as node C starts to transmit during the whole transmission duration of node A. Hence, we define the persistent collision zone as the area within the collision range of the receiver and outside the physical carrier sense range the transmitter, which is shown as the dotted area in **Fig. 1**.

3.3 Per-flow Throughput

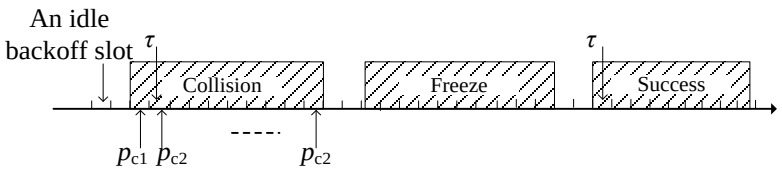

Fig. 2. Redefined performance metrics

With the notion of fixed length slot, all the performance metrics used are redefined. As shown in **Fig. 2**, the transmission probability τ is defined as the probability that the tagged node starts its transmission in a generic fixed length slot. The collision probability is the probability that one or more interfering nodes start their transmissions while the tagged node is transmitting a packet at a generic fixed length slot. As analyzed above, the collision probability in the first transmission slot is different from that in the remaining transmission slots. Here, we denote p_{c1} and p_{c2} as the collision probability in the first transmission slot and any one of the remaining transmission slot, respectively. The packet will be successfully received if it is not collided during the whole transmission process. Let p_s be the probability that the packet will be successfully received, and the per-flow throughput is given by

$$S = \frac{\tau p_s E[P]}{\sigma}. \tag{3}$$

4. Analytical Model

In this section, we propose a four-dimensional Markov chain model based on the notion of fixed length slot. To obtain the freezing probability $p_f(n)$ and the number of slots in a freezing process, $M(n)$, we leverage an iterative technique which is originally presented in [24]. More specifically, we first assume a Poisson point schedule process of each node and obtain the first guess of $p_f(n)$ and $M(n)$. Then with pf(n) and $M(n)$, we derive the per-flow throughput through our four-dimensional Markov chain model. Next, with the per-flow throughput, we update $p_f(n)$ and $M(n)$. New $p_f(n)$ and $M(n)$ are used again in the four-dimensional Markov chain model to calculate the per-flow throughput. Thus, the process is repeated until convergence is reached.

4.1 Fixed Length Slot Based Markov Chain Model

In the Markov chain model shown in **Fig. 3**, the state of the tagged node can be described as $\{i, j, k, l\}$, where

- j and k are defined as the random backoff processes representing the backoff stage and the value of the backoff counter, respectively. The backoff counter decrements at the end of each idle time slot. If the transmission fails, the backoff stage increases by 1 until to a specific retry limit. The backoff stage will be reset to 0 after a successful transmission or discarding of a packet due to the retry limitation.
- i has only four values (i = 0, 1, 2, 3) representing four different processes of the tagged node (i.e. the backoff process, successful transmission process, collision process, and freezing process, respectively).
- l represents the number of remaining slots in the current process. Hence, during the backoff process, l always equals to k.

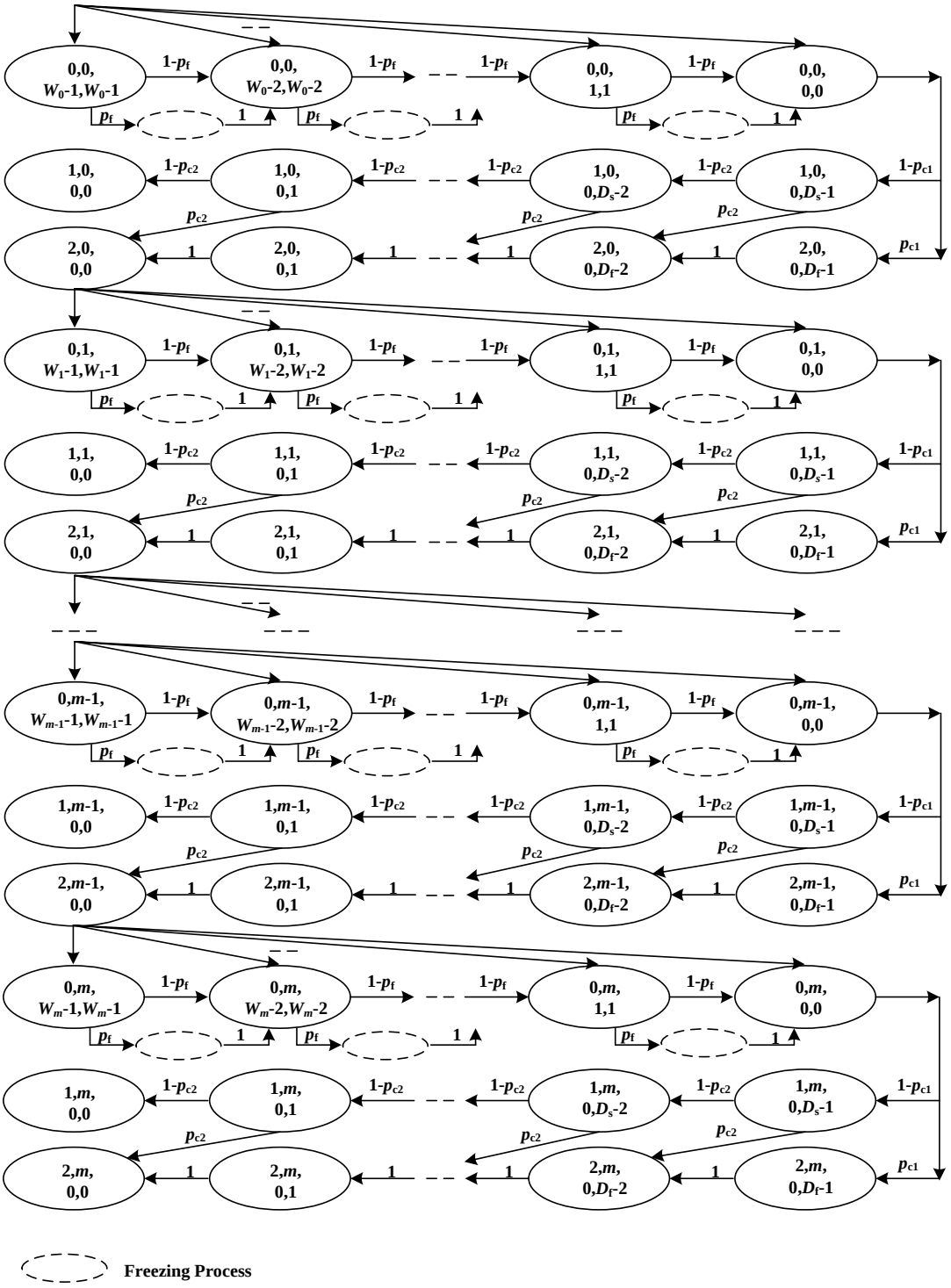

Fig. 3. The total Markov chain model for the tagged node

In the DCF protocol, a node senses the channel before transmitting a packet. As discussed above, we view the channel as a succession of fixed length slots, σ. If the channel is idle for a period of time equal to σ, we call it the backoff slot. Thus the backoff counter decrements at

the end of each backoff slot, which is referred to as the backoff process in this paper. However, when the channel is sensed busy, the node will freeze its backoff counter and start a freezing process (shown as the dotted line circle in **Fig. 3**) until the channel is sensed idle again. In this study, we assume that the tagged node starts the freezing process with probability, $p_f(n)$, for each backoff slot and the freezing process will last for $M(n)$ slots as shown in **Fig. 4**. After the freezing process ends, the tagged node will go to the next backoff slot with probability 1. When the backoff time counter reaches zero, the node will enter into either the collision process with a probability of $p_{c1}(n)$ or the successful transmission process with a probability of $1\text{-}p_{c1}(n)$. Note that the node can also go into the collision process with a probability of $p_{c2}(n)$ due to the persistent collisions at any slot of a successful transmission process. The packet is successfully received if and only if none of the slots in the successful transmission process is collided.

Although IEEE 802.11 DCF defines two channel access mechanisms, we only focus on the analysis of the basic access mechanism for two reasons: (1) the basic access mechanism is mandatory, whereas RTS/CTS handshaking mechanism is an optional variant; (2) The hidden terminal problem analyzed in this study still exists in the RTS/CTS handshaking mechanism. Furthermore, our work is ready to be extended to the RTS/CTS handshaking mechanism. In **Fig. 3**, D_s and D_f represent the number of slots for a successful transmission process and a collision process, respectively. Indeed, since the sending node relies on the reception of the ACK frame to determine if the packet is successfully received, both the successful transmission process and the collision process consist of D slots for the basic access mechanism.

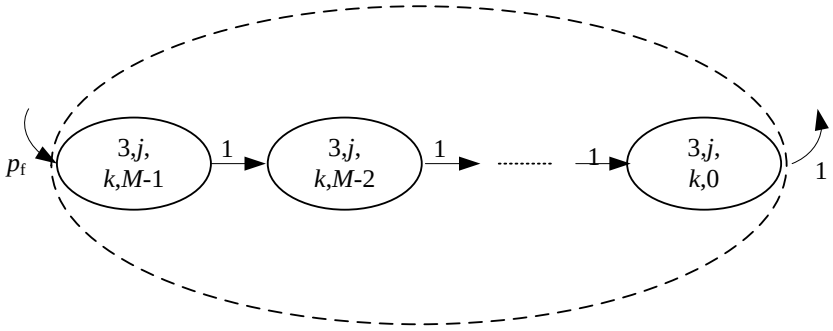

Fig. 4. The freezing process

After a failed transmission, the backoff stage increases, and the contention window (CW) size doubles until to the maximum size (CW_{max}). When the packet reaches a specific retry limit, it will be discarded and the backoff stage will be resumed to the initial backoff stage. Let W_i denote the contention window size of the ith backoff stage and m denote the retry limit, then CW_{max} can be simplified to W_{max}. Therefore, W_i can be expressed as

$$W_i = \begin{cases} 2^i W_0 & 0 \le i \le m', \\ W_{max} & m' < i \le m \end{cases}, \tag{4}$$

where $m' = \log_2(W_{max}/W_0)$.

For writing convenience, we define the transition probability from state "a" to state "b" as $p(b|a)$. Then based on the analysis above, the non null one-step transition probabilities of the model are

$$\begin{cases} p(0,j,k,k \mid 0,j,k+1,k+1) = 1-p_f(n) \quad 0 \le j \le m, 0 \le k \le W_j - 2 \\ p(3,j,k,M(n)-1 \mid 0,j,k,k) = p_f(n) \quad 0 \le j \le m, 1 \le k \le W_j - 1 \\ p(3,j,k,l \mid 3,j,k,l+1) = 1 \quad 0 \le j \le m, 1 \le k \le W_j - 1, 0 \le l \le M(n) - 2 \\ p(0,i,j,j \mid 3,i,j+1,0) = 1 \quad 0 \le i \le m, 0 \le j \le W_i - 2 \\ p(1,j,0,D-1 \mid 0,j,0,0) = 1-p_{c1}(n) \quad 0 \le j \le m \\ p(2,j,0,D-1 \mid 0,j,0,0) = p_{c1}(n) \quad 0 \le j \le m \\ p(1,j,0,l-1 \mid 1,j,0,l) = 1-p_{c2}(n) \quad 0 \le j \le m, 1 \le l \le D-1 \\ p(2,j,0,l-1 \mid 1,j,0,l) = p_{c2}(n) \quad 0 \le j \le m, 1 \le l \le D-1 \\ p(0,0,k,k \mid 1,j,0,0) = 1/W_0 \quad 0 \le j \le m, 1 \le k \le W_0 - 1 \\ p(0,j+1,k,k \mid 2,j,0,0) = 1/W_{j+1} \quad 0 \le j \le m-1, 0 \le k \le W_{j+1} - 1 \\ p(0,0,k,k \mid 2,m,0,0) = 1/W_0 \quad 0 \le k \le W_0 - 1 \end{cases} . \tag{5}$$

Next, we try to find a solution for the Markov chain. Let $p(i, j, k, l)$ be the probability of a node occupying the state $\{i, j, k, l\}$ at a generic slot. Actually, it is different for each sending node. For notational simplicity, we drop n from the expression $p_n(i, j, k, l)$. Based on the non null one-step transition probabilities analysis, for the backoff process, we note the following relation

$$p(0,j,k,k) = p(0,j,k+1,k+1) + \frac{(1-p_s(n))\,p(0,j-1,0,0)}{W_j} \quad (0 < k \le W_j - 2, 0 < j \le m). \tag{6}$$

For $k = W_j$-1, we have

$$p(0,j,W_j-1,W_j-1) = \frac{(1-p_s(n))\,p(0,j-1,0,0)}{W_j}, \tag{7}$$

where $p_s(n)$ is the probability that the packet will be successfully received by the destination node. Thus, we can obtain the probability of any state in the backoff process

$$p(0,j,k,k) = \frac{(W_j-k)(1-p_s(n))\,p(0,j-1,0,0)}{W_j} \quad (0 < k \le W_j - 1, 0 < j \le m). \tag{8}$$

Note that the backoff stage increases after a fail transmission until to a specific retry limit, i.e.,

$$p(0,j,0,0) = (1-p_s(n))\,p(0,j-1,0,0) \quad 1 \le j \le m. \tag{9}$$

Then, we can further express the probability of any state in the backoff process as a function of $p(0, 0, 0, 0)$

$$p(0,j,k,k) = \frac{(W_j-k)(1-p_s(n))^j\,p(0,0,0,0)}{W_j} \quad (0 < k \le W_j - 1, 0 \le j \le m). \tag{10}$$

Hence, for a generic slot, the probability of node n being in the backoff process is

$$A(n)=\sum_{j=0}^{m}\sum_{k=1}^{W_j-1}p(0,j,k,k)=\frac{p(0,0,0,0)}{2}\left[\frac{1-(2(1-p_s(n)))^{m+1}}{1-2(1-p_s(n))}W_0-\frac{1-(1-p_s(n))^{m+1}}{p_s(n)}\right]. \quad (11)$$

Since the node sends the packet when the backoff counter reaches zero, the transmission probability in a slot, $\tau(n)$, can be derived as

$$\tau(n)=\sum_{j=0}^{m}p(0,j,0,0). \quad (12)$$

It is an important metric for the performance evaluation of the IEEE 802.11 ad hoc network, and it will be used for calculating the collision probabilities.

From the second and the third equation in (5), we obtain the probability of any state in the freezing process as

$$p(3,j,k,l)=p_f(n)p(0,j,k,k)\quad 0\le j\le m,1\le k\le W_j-1,0\le l\le M(n)-1. \quad (13)$$

For the successful transmission process, we have

$$p(1,j,0,l)=\begin{cases}p(0,j,0,0)(1-p_{c1}(n)) & l=D-1\\ p(1,j,0,l+1)(1-p_{c2}(n)) & 0\le l<D-1\end{cases}, \quad (14)$$

where $j\in[0, m]$. The first equation in (14) represents that there is no collision at the first slot of the transmission process. The other equation in (14) denotes the fact that there is no persistent collision at any other slot of the successful transmission process. Hence, by means of equations (9) and (14), the probability that the tagged node is in the successful process at a generic slot is

$$\sum_{j=0}^{m}\sum_{l=0}^{D-1}p(1,j,0,l)=(1-p_{c1}(n))\frac{1-(1-p_{c2}(n))^D}{p_{c2}(n)}\frac{1-(1-p_s(n))^{m+1}}{p_s(n)}p(0,0,0,0). \quad (15)$$

For the collision process, we have

$$p(2,j,0,k)=\begin{cases}p(0,j,0,0)p_{c1}(n) & k=D-1\\ p_{c2}(n)\sum_{l=k+1}^{D-1}p(1,j,0,l)+p(2,j,0,D-1) & 0\le k<D-1\end{cases}, \quad (16)$$

where $j\in[0, m]$. It represents that node n can go into the collision process from either the backoff process with a probability of $p_{c1}(n)$ or the successful transmission process with a probability of $p_{c2}(n)$. Then by substituting equation (9) into equation (16), we can derive the probability that node n remains in the collision process as follows

$$\sum_{j=0}^{m}\sum_{l=0}^{D-1}p(2,j,0,l)=(D-(1-p_{c1}(n))\frac{1-(1-p_{c2}(n))^D}{p_{c2}(n)})\frac{1-(1-p_s(n))^{m+1}}{p_s(n)}p(0,0,0,0). \quad (17)$$

Thus, the probability that the tagged node is in the transmission process in a generic slot can be expressed as

$$\tau'(n)=\sum_{j=0}^{m}\sum_{l=0}^{D-1}p(1,j,0,l)+\sum_{j=0}^{m}\sum_{l=0}^{D-1}p(2,j,0,l). \tag{18}$$

By adopting the normalization condition, we have

$$\sum_{j=0}^{m}\sum_{k=1}^{W_j-1}p(0,j,k,k)+\sum_{j=0}^{m}\sum_{l=0}^{D-1}p(1,j,0,l)+\sum_{j=0}^{m}\sum_{l=0}^{D-1}p(2,j,0,l)+\sum_{j=0}^{m}\sum_{k=1}^{W_j-1}\sum_{l=0}^{M(n)-1}p(3,j,k,l)=1. \tag{19}$$

For writing convenience, we assume

$$p_1=\frac{\left(1+M(n)p_f(n)\right)}{2}, \tag{20}$$

$$p_2=D\frac{1-(1-p_s(n))^{m+1}}{p_s(n)}. \tag{21}$$

Then, substituting equations (10), (11), (13), (15) and (17) into equation (19), we can obtain

$$p(0,0,0,0)=\begin{cases}\dfrac{1}{p_1\left[\dfrac{1-2^{m+1}(1-p_s(n))^{m+1}}{2p_s(n)-1}W_0-\dfrac{1-(1-p_s(n))^{m+1}}{p_s(n)}\right]+p_2} & m\le m'\\ \dfrac{1}{p_1\left[\dfrac{1-(2-2p_s(n))^{m'+1}}{2p_s(n)-1}W_0-\dfrac{1-(1-p_s(n))^{m+1}}{p_s(n)}+\dfrac{(W_{\max}-1)(1-p_s(n))^{m'+1}\left(1-(1-p_s(n))^{m-m'}\right)}{p_s(n)}\right]+p_2} & m>m'\end{cases}. \tag{22}$$

Given the length of the packet, D can be obtained as

$$D=(H+\mathrm{E}[P]+\mathrm{SIFS}+ACK)/\sigma, \tag{23}$$

where H, E[P], and ACK represent the time period the node needs to transmit the MAC and PHY frame header, the packet, and the ACK frame, respectively.

4.2 Collision Probabilities

As discussed above, we note that when d is larger than $0.79r_{tx}$, the collision range of the receiver exceeds the physical carrier sense range of the transmitter thus leading to two different kinds of collisions. Here, we aim to calculate the collision probability at the first slot of the transmission process, p_{c1}, and the collision probability at any other slot of the transmission process, p_{c2}.

Let ZI and ZP denote the set of transmitters in the instantaneous collision zone and the persistent collision zone, respectively. As shown in **Fig. 1**, the transmitter of flow 1 (node A) wants to transmit a packet to its receiver (node B). When the backoff counter of node A reaches zero, collisions will occur at node B if any other transmitter within its instantaneous collision range (i.e. node C) simultaneously transmits a frame or transmitters in the persistent

collision zone (i.e., node D) are in the transmission process. In addition, if there are flows of which the transmitters are out of the physical carrier sense range of node A and the collision range of node B while the receivers are in the collision range of node B (i.e., node E), collisions can also occur due to the transmission of the ACK frames. Denote *ZA* as the set of the transmitters of these flows. Then, the collision probability of node *n*, $p_{c1}(n)$ can be calculated by

$$p_{c1}(n) = 1 - \prod_{\substack{i \in ZI,\, j \in ZP,\\ k \in ZA}} (1-\tau(i))(1-\tau'(j))(1-\tau(k)p_s(k)). \tag{24}$$

Since a receiver responds with the ACK frame upon receiving the packets successfully regardless of the channel state, both the collisions due to the transmitters in the persistent collision zone and the collisions due to the ACK frames exist during the whole transmission process. The collision probability $p_{c2}(n)$ can be obtained as

$$p_{c2}(n) = 1 - \prod_{i \in ZP,\, j \in ZA} (1-\tau(i))(1-\tau(j)p_s(j)). \tag{25}$$

Hence, the instantaneous collision zone and the persistent collision zone only refer to the sending nodes. For simplicity, we assume that the ACK frame can be transmitted in a slot and can be successfully received since it is much shorter than the Data frame. The packet will be successfully received only if none of the slots is collided during the whole transmission process. Therefore, we have the successful probability, $p_s(n)$

$$p_s(n) = (1-p_{c1}(n))(1-p_{c2}(n))^{D-1} \quad . \tag{26}$$

4.3 The Freezing Process

Up to now, it turns out that the only unknown variables are the freezing probability $p_f(n)$ and the number of slots in a freezing process, $M(n)$. Here, we compute them through an iterative way which is originally proposed in [24]. The authors in [24] employed the continuous time Markov chain model to obtain the fraction of time during which the tagged node can potentially start to transmit. In the continuous time Markov chain model, the tagged node (i.e., node *n*) is assumed to transmit packets according to a Poisson point process with a rate of $g(n)$ and the average length of packets transmitted from node *n* is $1/u(n)$. Each state of the continuous time Markov chain is a set of links that can coexist due to the spatial reuse property of the wireless medium. The steady-state probability can be expressed as

$$Q(B) = \left(\prod_{n \in B} \frac{g(n)}{\mu(n)} \right) Q(\phi), \tag{27}$$

where $Q(\Phi)$ is the probability that there is no node transmitting a packet. Normalizing equation (27), we obtain

$$Q(\phi) = [\sum_{all\ B} \prod_{i \in B} \frac{g(n)}{u(n)}]^{-1}. \tag{28}$$

Since node n is assumed to schedule its transmissions according to a Poisson point process, we obtain the probability that no scheduling event starts while node n can transmit during a time interval σ as $e^{-G(n)\sigma}$. In the four-dimensional Markov chain model, the probability can be expressed as $(1-\tau(n))(1-p_f(n))$. Thus, we have

$$p_f(n) = 1 - \frac{e^{-G(n)\sigma}}{1-\tau(n)}, \tag{29}$$

where $G(n)$ denotes the aggregate scheduling rate while node n can transmit i.e.,

$$G(n) = g(n) + \sum_{n' \in C(n)} A(n' \mid n)\, g(n'), \tag{30}$$

where $A(n'|n)$ represents the probability that one of its neighbors, say n', is allowed to transmit, conditioned on the fact that n can transmit. Let $\overline{N}(n)$ represent the set of all transmitters that locate outside the physical carrier sense range of node n, $A(n'|n)$ can be derived as

$$A(n' \mid n) = \frac{A(n', n)}{A(n)} = \frac{\sum_{H \subset \overline{N(n) \cup N(n')}} \left(\prod_{i \in H} \frac{g(i)}{u(i)}\right)}{\sum_{H \subset \overline{N}(n)} \left(\prod_{i \in H} \frac{g(i)}{u(i)}\right)}. \tag{31}$$

The probability of the channel around node n being sensed idle can be expressed as

$$A(n) = \sum_{H \subset \overline{N}(n)} Q(H) = \frac{\sum_{H \subset \overline{N}(n)} \left(\prod_{i \in H} g(i)/u(i)\right)}{\sum_{all\, H} \left(\prod_{i \in H} g(i)/u(i)\right)}. \tag{32}$$

We then establish the relationship between the continuous time Markov model and the fixed slot time based Markov chain model as shown in equations (11), (29) and (32). Given an initial guess of $g(n)$ and $u(n)$, we can calculate $p_f(n)$ and $A(n)$ through equations (29) and (32), respectively. Then, with $A(n)$, we can obtain $M(n)$ by means of equation (11). With $p_f(n)$ and $M(n)$, the per-flow throughput $s(n)$ can be calculated through equation (3). Since the packet will be successfully received if there is no persistent collision when the nodes in the physical carrier sense range of node n are not transmitting, the throughput of node n can also be expressed as

$$s(n) = A(n)g(n)(1 - p_{c2}(n)). \tag{33}$$

Equation (33) can thus be used to update $g(n)$. Then all the variables such as $pf(n)$, $\tau(n)$, $p_{c1}(n)$, $p_{c2}(n)$, $p_s(n)$, etc. in the fixed slot based Markov chain model can be updated accordingly. Note that the variables are used in turn in equation (3) to calculate a new per-flow throughput $s(n)$ again. Thus, the procedure continues until convergence is reached.

5. Model validations and Analysis

In order to validate the model, we have compared the analytical results with the simulation results obtained by the QualNet simulator. We consider the topology where 30 flows randomly distributed in a square of 2000×2000m, as shown in **Fig. 5**. The solid lines denote the transmission pairs and the dotted lines connect the sending nodes that are in the physical carrier sense range of each other. The transmitter of the nth flow is denoted as node *n*. The transmission range and physical carrier sense range are set to 250m and 530m, respectively. Without loss of generality, we set the distance between the transmitter and its receiver to 200m for each flow. Then, we can obtain that the collision range for each receiver is approximate to 356m by means of equation (2). Each node always has at least one packet to send and the payload from the application layer is fixed at 256 bytes. Other parameters used to obtain the analytical results and simulation results are summarized in **Table 1**.

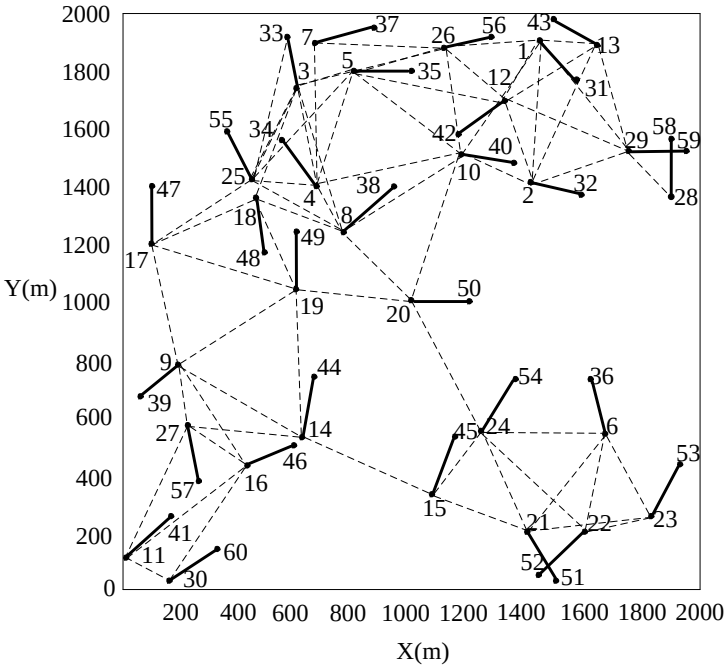

Fig. 5. A random topology of 30 flows

Table 1. The simulation parameters

Parameter	Value	Parameter	Value
Total number of nodes	60	SIFS	10us
Channel Bandwidth	2Mbps	Propagation Model	Two-Ray
Length of PHY Header	192bits	SINR Threshold	10dB
Length of MAC Header	224bits	Simulation Time	50s
Time Slot	20us	Propagation limit	-87dBm

5.1 Transmission Probabilities

Fig. 6 shows the analytical and simulation transmission probabilities of each flow. It can be seen that the simulation results and the analytical results are approximately matched well. We

note that the transmission probabilities of the flows differ from each other significantly. Indeed, before each transmission, nodes may spend some time on the backoff process and the freezing process. The less time nodes spend on them, the higher transmission probabilities will be obtained. **Fig. 7** and **Fig. 8** show the analytical and simulation results of the probabilities that the nodes stay in the freezing process and the backoff process, respectively.

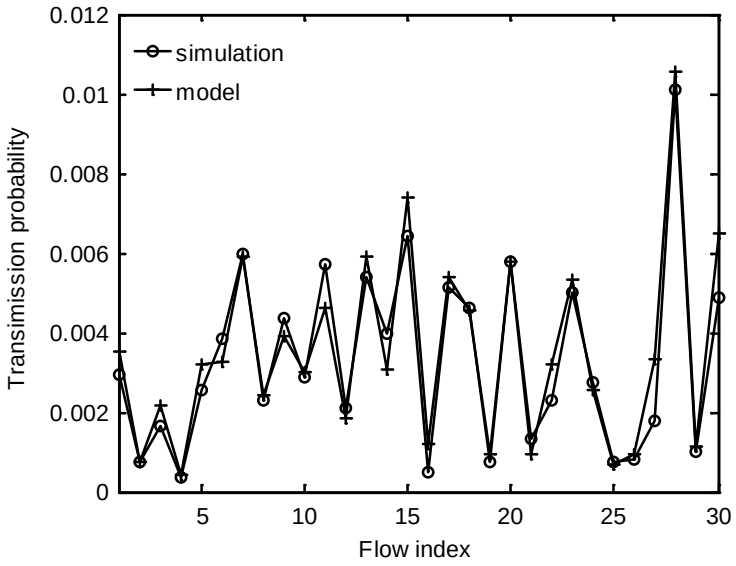

Fig. 6. Transmission probability of each flow

In simulation, we measure the probability that the tagged node remains in the freezing process as the fraction of time each sending node spends on the freezing process. Let p_f' denote the probability that the tagged node is in the freezing process in a slot, it can be calculated as

$$p_f' = \sum_{i=0}^{m} \sum_{j=1}^{W_i-1} \sum_{l=0}^{Q-1} p(3,i,j,l) . \tag{34}$$

This is mainly depended on the behavior of the nodes that locate in the physical carrier sense range and is less affected by the collisions the tagged node has experienced. We can see that the probability of node 28 being in the freezing process is rather low because it has only one node in its physical carrier sense range.

Fig. 8 shows simulation and analytical results of the probability of node i (i=1, 2,…30) being in the backoff process, denoted as $A(i)$ in this paper. This quantity can be calculated by means of equation (11). In **Fig. 9**, the probabilities of the nodes in the backoff progress under different contention window sizes. As expected, this probability increases as the initial contention window size increases. As a result, the transmission probabilities will decrease when the initial contention window size increases for the most flows. In addition, since the transmissions of other nodes in the physical carrier sense range also make the tagged node defer its transmission, the transmission probabilities of some nodes can also increase due to the decrease of the transmission probabilities of the nodes in their physical carrier sense range.

Another interesting finding is that for the most flows that achieve higher transmission opportunity, the probabilities that they are in the backoff progress are higher. Hence, we can

see that the transmission probabilities of these flows get lower when the initial contention window size increases because they spend more time on the backoff progress as shown in **Fig. 10**. Meanwhile, flows will spend less time on the freezing process when the transmission probabilities of other flows get lower as shown in **Fig. 10**. As a result, the transmission probabilities of the flows will get higher. Hence, we can see it from **Fig. 11** that some flows get lower transmission probabilities while other flows get higher transmission probabilities when the initial contention window size increases.

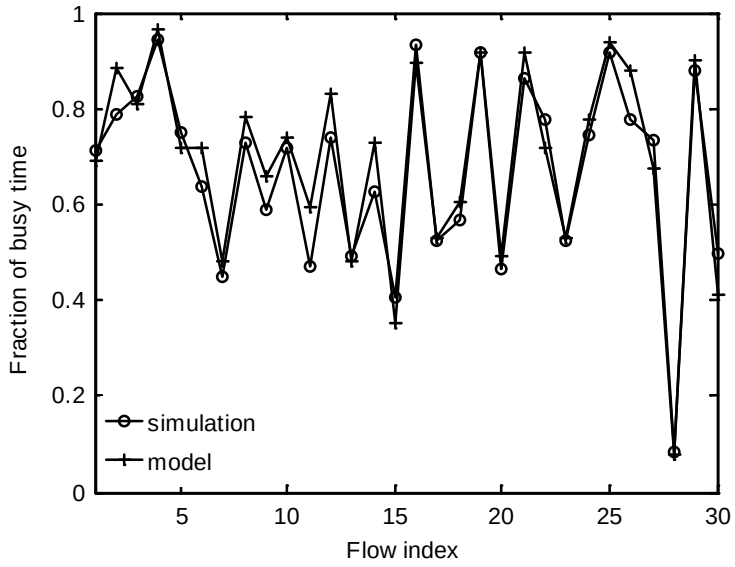

Fig. 7. The probability of the tagged node being in the freezing process

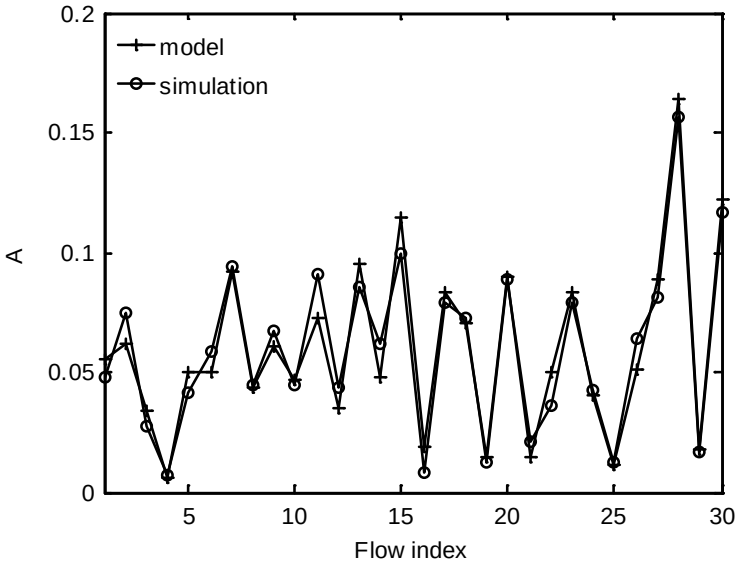

Fig. 8. The probability of the nodes being in the backoff process

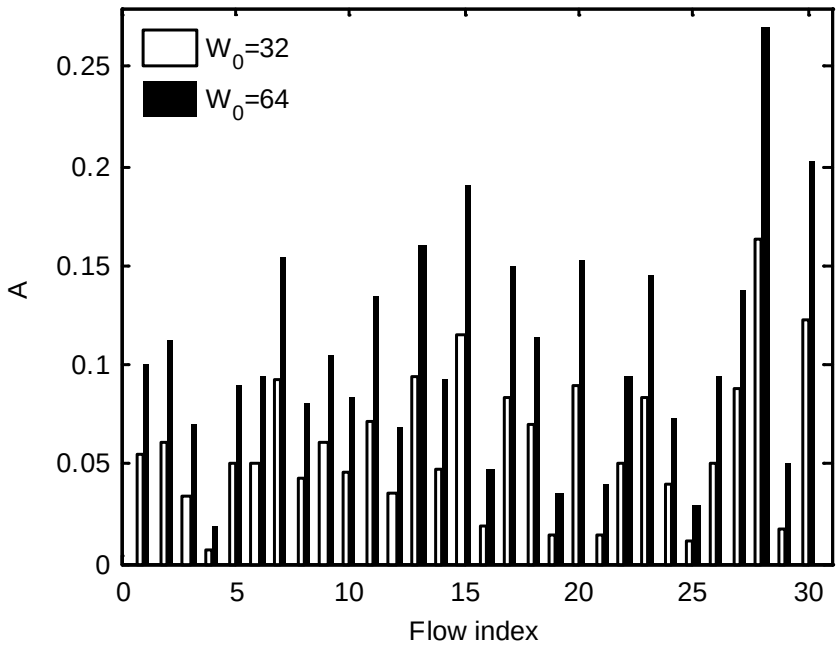

Fig. 9. The probabilities of the nodes being in the backoff progress

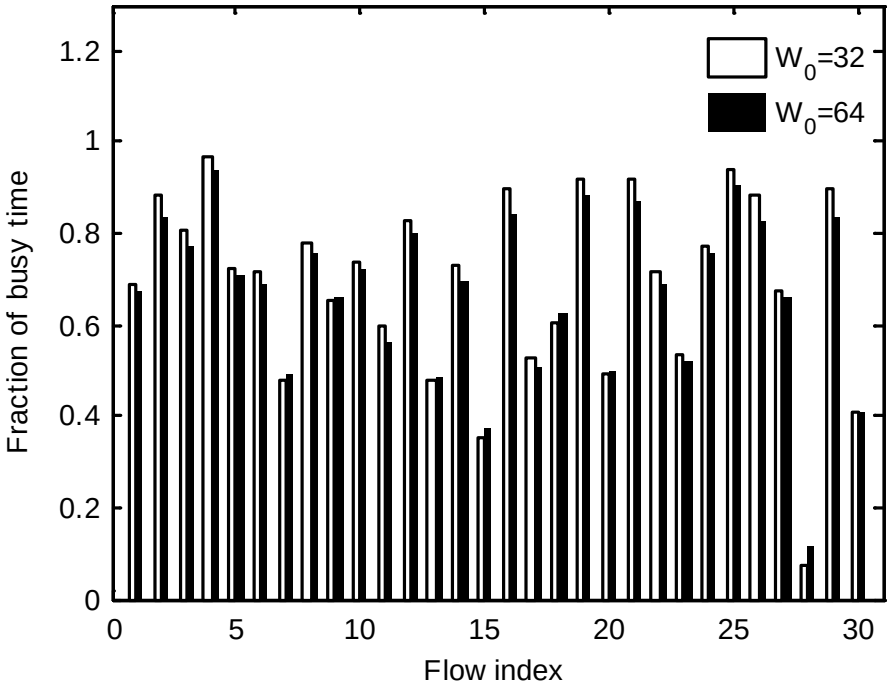

Fig. 10. The probabilities of the nodes being in the freezing progress

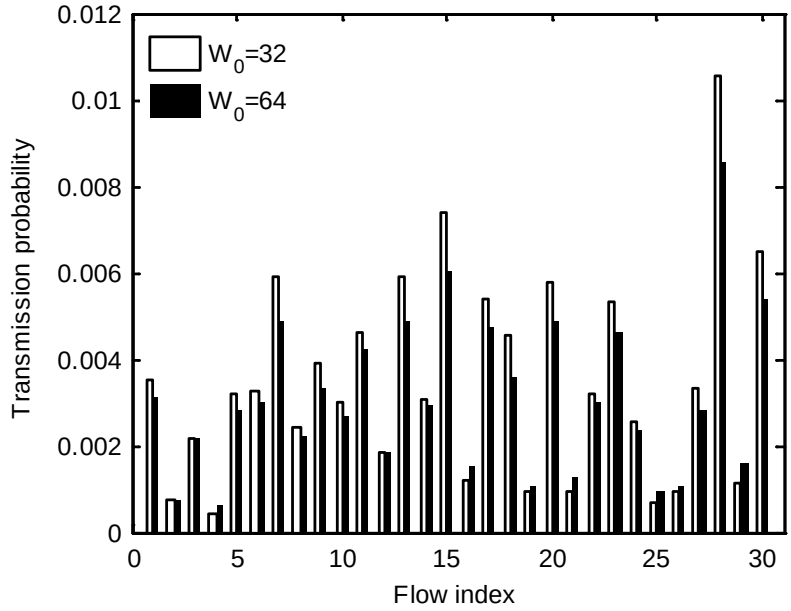

Fig. 11. Transmission probabilities

5.2 Collision Probabilities

The simulation and analytical results of the collision probability of each flow are shown in **Fig. 12**. Note that the six flows that have much higher collision probability than other flows all suffer from persistent collisions. **Table 2** shows the analytical instantaneous and persistent collision probabilities of the six flows.

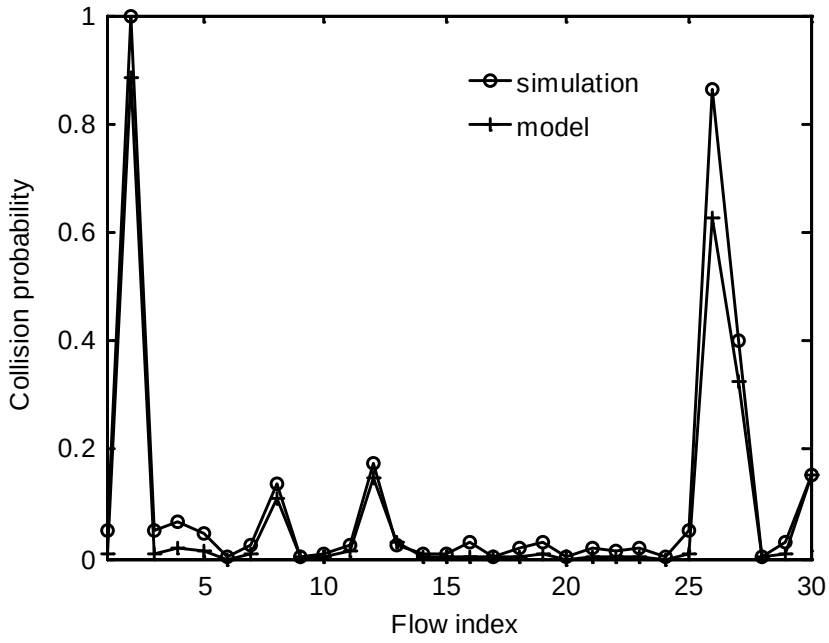

Fig. 12. Collision probability of each flow

Table 2. The instantaneous and persistent collision probabilities

Flow index	2	8	12	26	27	30
Instantaneous collision	0.0945	0.0034	0.0047	0.0012	0.0054	0.0058
Persistent collision	0.7880	0.1064	0.1427	0.6202	0.3230	0.1461

As analyzed above, the collision probability of the tagged node depends on the transmission probabilities of the interference nodes. Node 28 and node 13 locate in the persistent collision zone of node 2 and node 26, respectively. Since node 28 has a higher transmission probability than node 13 as shown in **Fig. 6**, we can see that the collision probability of node 2 is higher than node 26. The persistent collisions of the other four flows are induced by the interfering ACK frames. The ACK frames are transmitted only when the Data frames are received successfully. Besides, the transmission probabilities of node 28 and node 13 are higher than other interfering nodes. Hence, the transmission probabilities of the ACK frames are usually much lower than that of the Data frames from node 28 and node 13. As a result, the persistent collision probabilities caused by them are much lower. **Fig. 13** shows the collision probabilities of the six flows when different initial contention window sizes are used. We can find that the collision probabilities of some flows decrease while some others increase a bit, which can also be explained with the transmission probabilities of their interfering nodes.

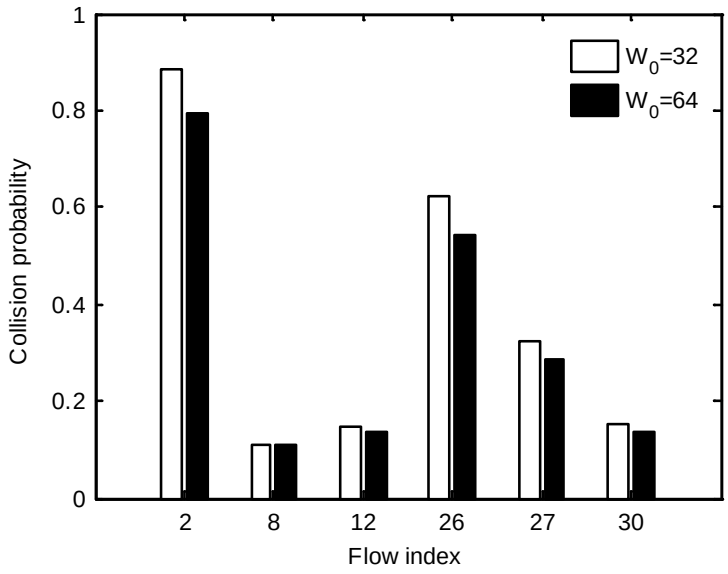

Fig. 13. Collision probabilities

5.3 Per-flow Throughput

Fig. 14 shows the analytical and simulation results of the saturation throughput of each flow. From the figure, we note that some flows can achieve very high throughput while some other flows get starved due to serious collisions or the lack of opportunity to transmit. The transmission probability and the collision probability are considered as the two fundamental factors that affect the throughput. Note that node 18 has a much higher transmission probability than node 19 as shown in Fig. 6. Hence, we can see that the 18th flow achieves higher throughput than the 19th flow as shown in **Fig. 14** though they have almost the common nodes in their respective instantaneous collision zones and no node in their persistent collision zones. Meanwhile, note that the 28th flow has a very high transmission probability and rather

low collision probability, as shown in **Fig. 6** and **Fig. 12**. Hence, we can find that the 28th flow achieves rather high throughput.

In **Fig. 15**, we plot the per-flow throughputs under two different contention window sizes. We find that when the contention window size increases, the throughputs of the flows that achieve high throughputs are decreased while the throughputs of the flows that achieve low throughputs are increased. This is because that the transmission probabilities of the dominating flows decrease with the increase of the contention window size, and thus provides more opportunity to other flows to transmit their packets. Besides, the collision probabilities of the flows that suffer from serious collisions are also decreased as shown in **Fig. 13**.

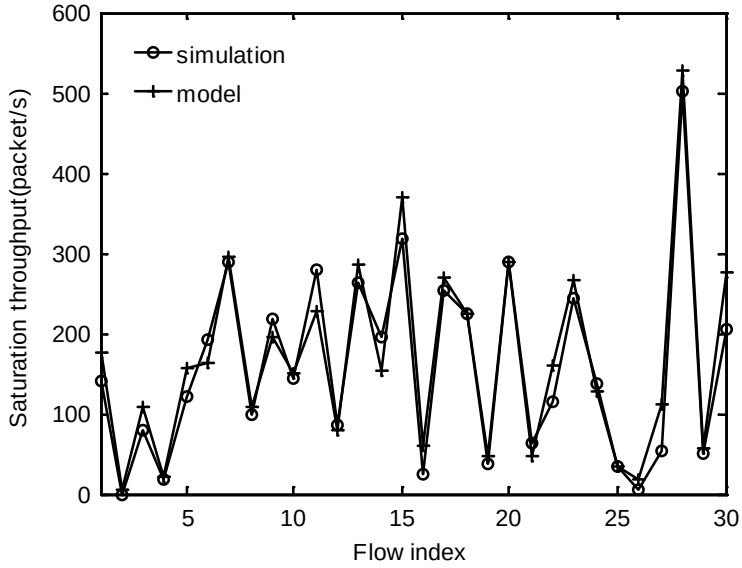

Fig. 14. Saturation throughput of each flow

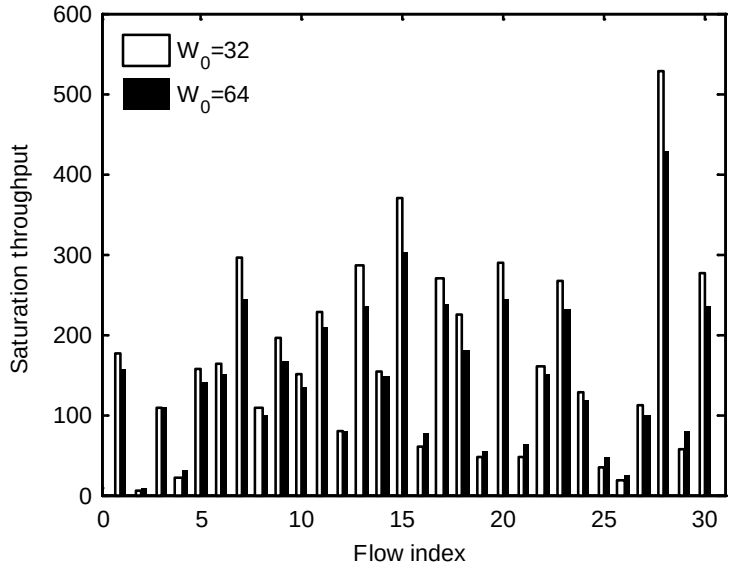

Fig. 15. Throughputs of each flow

6. Conclusions and Future Work

In this paper, we show that there are two different kinds of collisions in the whole transmission process, which are referred to as the instantaneous collisions and persistent collisions. Then we propose a four-dimensional Markov chain model based on the fixed length channel slot to analyze the MAC layer throughput of each flow in IEEE 802.11 multi-hop ad hoc networks. Through the model, the transmission probability, the collision probability and the throughput of each flow based on the notion of fixed length channel slot are derived. By comparing the analytical results with the simulation results, we validate the accuracy of our model. Through a further study on the transmission probability, the collision probability, and the throughput of each flow, we also find that the unfairness problem in multi-hop net works can be alleviated by increasing the contention windows for each flow.

In our future work, we will extend the model to design optimal backoff parameters to avoid the unfairness problem. We are also investigating the performance of each flow in IEEE 802.11 multi-hop ad hoc networks with heterogeneous parameters (the transmit power level, transmit rate, etc).

References

[1] D. Benyamina, A. Hafid, and M. Gendreau, "Wireless mesh networks design - a survey," *IEEE Communications Surveys & Tutorials*, vol. 14, no. 2, pp. 299-310, May 2012. Article (CrossRef Link)

[2] I. F. Akyildiz and X. Wang, "A survey on wireless mesh networks," *IEEE Communications Magazine*, vol. 43, no. 9, pp. S23-S30, Sept. 2005. Article (CrossRef Link)

[3] L. Zhou, Z. Yang, H. Wang, and M. Guizani, "Impact of execution time on adaptive wireless video scheduling," *IEEE Journal on Selected Areas in Communications*, vol. 32, no. 4, pp. 760-772, Apr. 2014. Article (CrossRef Link)

[4] L. Zhou, "Mobile device-to-device video distribution: theory and application," *ACM Transactions on Multimedia Computing, Communications and Applications*, vol. 12, no. 3, pp. 1253-1271, June 2016. Article (CrossRef Link)

[5] G. Bianchi, "Performance analysis of the IEEE 802.11 distributed coordination function," *IEEE Journal on Selected Areas in Communications*, vol. 18, no. 3, pp. 535-547, Mar. 2000. Article (CrossRef Link)

[6] E. Ziouva and T. Antonakopoulos, "CSMA/CA performance under high traffic conditions: throughput and delay analysis," *Computer Communications*, vol. 25, no. 3, pp. 313-321, Feb. 2002. Article (CrossRef Link)

[7] C. H. Foh and J. W. Tantra, "Comments on IEEE 802.11 saturation throughput analysis with freezing of backoff counters," *IEEE Communications Letters*, vol. 9, no. 2, pp. 130-132, Feb. 2005. Article (CrossRef Link)

[8] I. Tinnirello, G. Bianchi, and Y. Xiao, "Refinements on IEEE 802.11 distributed coordination function modeling approaches," *IEEE Transactions on Vehicular Technology*, vol. 59, no. 3, pp. 1055-1067, Mar. 2010. Article (CrossRef Link)

[9] E. Felemban and E. Ekici, "Single hop IEEE 802.11 DCF analysis revisited: accurate modeling of channel access delay and throughput for saturated and unsaturated traffic cases," *IEEE Transactions on Wireless Communications*, vol. 10, no. 10, pp. 3256-3266, Oct. 2011. Article (CrossRef Link)

[10] K. Ghaboosi, B. H. Khalaj, Y. Xiao, and M. Latva-aho, "Modeling IEEE 802.11 DCF using parallel space–time Markov chain," *IEEE Transactions on Vehicular Technology*, vol. 57, no. 4, pp. 2404-2413, July 2008. Article (CrossRef Link)

[11] F. Calì, M. Conti, and E. Gregori, "Dynamic tuning of the IEEE 802.11 protocol to achieve a theoretical throughput limit," *IEEE/ACM Transactions on Networking*, vol. 8, no. 6, pp. 785-799, Dec. 2000. Article (CrossRef Link)
[12] Y. C. Tay and K. C. Chua, "A capacity analysis for the IEEE 802.11 MAC protocol," *Wireless Networks*, vol. 7, no. 2, pp. 159-171, Mar. 2001. Article (CrossRef Link)
[13] G. Bianchi and I. Tinnirello, "Remarks on IEEE 802.11 DCF performance analysis," *IEEE Communications Letters*, vol. 9, no. 8, pp. 765-767, Aug. 2005. Article (CrossRef Link)
[14] B.-J. Kwak, N.-O. Song, and L. E. Miller, "Performance analysis of exponential backoff," *IEEE/ACM Transactions on Networking*, vol. 13, no. 2, pp. 343-355, Apr. 2005. Article (CrossRef Link)
[15] T. Sakurai and H. L. Vu, "MAC access delay of IEEE 802.11 DCF," *IEEE Transactions on Wireless Communications*, vol. 6, no. 5, pp. 1702-1710, May 2007. Article (CrossRef Link)
[16] A. Rahman and P. Gburzynski, "Hidden problems with the hidden node problem," in *Proc. of 23rd Biennial Symposium on Communications*, pp. 270-273, 2006. Article (CrossRef Link)
[17] S. Xu and T. Saadawi, "Does the IEEE 802.11 MAC protocol work well in multihop wireless ad hoc networks?," in *Proc. of IEEE Communications Magazine*, vol. 39, no. 6, pp. 130-137, Jun. 2001. Article (CrossRef Link)
[18] G. Anastasi, E. Borgia, M. Conti, and E. Gregori, "IEEE 802.11b ad hoc networks: performance measurements," *Cluster Computing*, vol. 8, no. 2-3, pp. 135-145, July 2005. Article (CrossRef Link)
[19] D. Hoang and R. A. Iltis, "Performance evaluation of multi-hop CSMA/CA networks in fading environments," *IEEE Transactions on Communications*, vol. 56, no. 1, pp. 112-125, Jan. 2008. Article (CrossRef Link)
[20] J. He and H. K. Pung, "Performance modelling and evaluation of IEEE 802.11 distributed coordination function in multihop wireless networks," *Computer Communications*, vol. 29, no. 9, pp. 1300-1308, May 2006. Article (CrossRef Link)
[21] A. A. Abdullah, F. Gebali, and L. Cai, "Modeling the throughput and delay in wireless multihop ad hoc networks," in *Proc. of IEEE Global Telecommunications Conference*, pp. 1-6, Nov. 30 - Dec. 4, 2009. Article (CrossRef Link)
[22] R. Boorstyn, A. Kershenbaum, B. Maglaris, and V. Sahin, "Throughput analysis in multihop CSMA packet radio networks," *IEEE Transactions on Communications*, vol. 35, no. 3, pp. 267-274, Mar. 1987. Article (CrossRef Link)
[23] X. Wang and K. Kar, "Throughput modelling and fairness issues in CSMA/CA based ad-hoc networks," in *Proc. of IEEE 24th Annual Joint Conference of the IEEE Computer and Communications Societies*, pp. 23-34, March 13-17, 2005. Article (CrossRef Link)
[24] M. Garetto, T. Salonidis, and E. W. Knightly, "Modeling per-flow throughput and capturing starvation in CSMA multi-hop wireless networks," *IEEE/ACM Transactions on Networking*, vol. 16, no. 4, pp. 864-877, Aug. 2008. Article (CrossRef Link)
[25] A. Tsertou and D. I. Laurenson, "Revisiting the hidden terminal problem in a CSMA/CA wireless network," *IEEE Transactions on Mobile Computing*, vol. 7, no. 7, pp. 817-831, July 2008. Article (CrossRef Link)
[26] K.-L. Hung and B. Bensaou, "Throughput analysis and rate control for IEEE 802.11 wireless LAN with hidden terminals," in *Proc. of the 11th international symposium on Modeling, analysis and simulation of wireless and mobile systems*, pp. 140-147, October 27–31, 2008. Article (CrossRef Link)
[27] K. Ghaboosi, M. Latva-aho, Y. Xiao, and B. H. Khalaj, "Modeling nonsaturated contention-based IEEE 802.11 multihop ad hoc networks," *IEEE Transactions on Vehicular Technology*, vol. 58, no. 7, pp. 3518-3532, Sept. 2009. Article (CrossRef Link)

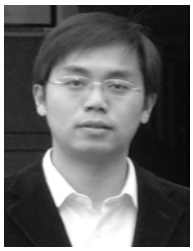

Lei Lei received the Bachelor Degree in electronic and information technology from Northwestern Polytechnical University in 2002, and the Ph.D. degree in communication and information system from Nanjing University of Aeronautics and Astronautics in 2008. Now, he is an associate professor in the College of Electronic and Information Engineering, Nanjing University of Aeronautics and Astronautics. His current research interests are in ad hoc networks and cooperative communications.

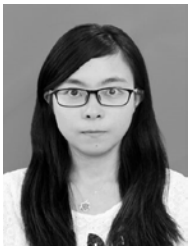

Xinru Zhao received the bachelor degree in electronic and information engineering from Nanjing University of Aeronautics and Astronautics in July 2015. She is currently working toward his master degree at the College of Electronic and Information Engineering, Nanjing University of Aeronautics and Astronautics. His research interests are in the area of ad hoc networks.

Shengsuo Cai received his M.Sc. degree major at communication engineering from Nanjing University of Aeronautics and Astronautics in 2014. He is now with the College of Electronic and Information Engineering, Nanjing University of Aeronautics and Astronautics of China. His research interests include the design and performance analysis of the MAC protocol for wireless ad hoc networks.

Xiaoqin Song received her Ph.D. degree major at communication engineering from Southeast University in 2007. She is now with the College of Electronic and Information Engineering, Nanjing University of Aeronautics and Astronautics of China. Her research interests mainly focus on cooperation communication and cognitive radio.

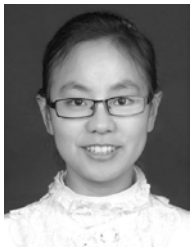

Ting Zhang received the bachelor degree in electronic and information engineering from the Nanchang Institute of Technology in July 2012.She is currently working toward his master degree at the College of Electronic and Information Engineering, Nanjing University of Aeronautics and Astronautics. Her research interests are in the area of wireless ad hoc networks.